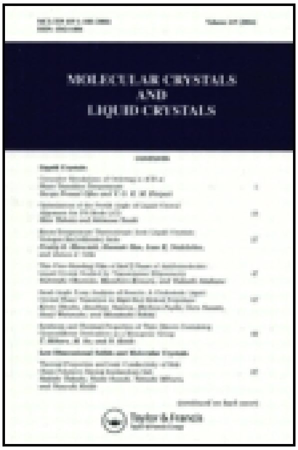

Molecular Crystals and Liquid Crystals
Publication details, including instructions for authors and subscription information:
http://www.tandfonline.com/loi/gmcl20

Nonlinear Exciton Relaxation in Ladder-Type Poly (Para-Phenylene)

V. Gulbinas [a] , I. Mineviciute [a] , D. Hertel [b] , R. Wellander [c] , A. Yartsev [c] & V. Sundstrom [c]

[a] Institute of Physics, Vilnius, Lithuania
[b] Institute of Physical Chemistry, University of Cologne, Cologne, Germany
[c] Lund University, Lund, Sweden

Version of record first published: 22 Sep 2010

To cite this article: V. Gulbinas, I. Mineviciute, D. Hertel, R. Wellander, A. Yartsev & V. Sundstrom (2007): Nonlinear Exciton Relaxation in Ladder-Type Poly (Para-Phenylene), Molecular Crystals and Liquid Crystals, 467:1, 47-57

To link to this article: http://dx.doi.org/10.1080/15421400701220890

Mol. Cryst. Liq. Cryst., Vol. 467, pp. 47–57, 2007

ISSN: 1542-1406 print/1563-5287 online
DOI: 10.1080/15421400701220890

Nonlinear Exciton Relaxation in Ladder-Type Poly (Para-Phenylene)

V. Gulbinas
I. Mineviciute
Institute of Physics, Vilnius, Lithuania

D. Hertel
Institute of Physical Chemistry, University of Cologne,
Cologne, Germany

R. Wellander
A. Yartsev
V. Sundstrom
Lund University, Lund, Sweden

Nonlinear exciton relaxation processes, exciton-exciton annihilation, and amplified spontaneous emission were investigated in thin films of ladder-type poly-(para-phenylene) under excitation by femtosecond light pulses. Both processes become apparent at similar excitation intensities, however their properties are very different. They cause different exciton relaxation kinetics and their intensity dependences are different.

Keywords: annihilation; ASE; conjugated polymer; femtosecond

INTRODUCTION

Excitons play a very important role in the operation of polymer-based photoelectric devices. This is because the interaction of a charge carrier and photons takes place via the exciton state. Therefore, the properties of excitons and, in particular, their lifetime are very important parameters determining the operation efficiency of organic

---

The investigation was partly supported by the Lithuanian State Foundation for Science and Studies. We thank Prof. Scherf for placing MeLPPP at our disposal.

Address correspondence to V. Gulbinas, Institute of Physics, Savanoriu 231, Vilnius, Lithuania. E-mail: vidgulb@ktl.mii.lt

light-emitting diodes and photoelectrical elements. Exciton lifetime in conjugated polymers is determined by both the chemical polymer structure and by the presence of various exciton quenching centers in a material.

Nonlinear exciton relaxation becomes important, when devices are operating under high light intensity conditions, like in polymeric lasers. On the other hand, the majority of the optical investigations of conjugated polymers are performed by using lasers under high light excitation conditions. Therefore, nonlinear relaxation processes may affect their results. Exciton-exciton annihilation is a commonly observed nonlinear relaxation process in condensed organic materials [1,2]. Usually, it becomes important at the material excitation by laser pulses of resonant light with intensity of the order of hundreds of mJ/cm^2 and leads to an increase of the exciton relaxation rate and a reduction of the fluorescence yield. The amplified spontaneous emission (ASE) [3–6] is another nonlinear relaxation process which is less frequently observed. However, it can be observed in some cases at lower intensities and can be more effective than the exciton-exciton annihilation [3]. This process is closely related to the laser performance; therefore, it was also widely investigated.

Although both the discussed nonlinear relaxation processes lead to the faster exciton relaxation, their influences are rather different. From the formal point of view, the exciton-exciton annihilation increases the nonradiative relaxation rate, whereas the ASE increases the radiative relaxation rate. Therefore, the former leads to a reduction of the fluorescence quantum yield, whereas the latter to its increase. The exciton-exciton annihilation is related to the energy transfer via the Förster process. The transfer rate depends on the distance between exciton donor and acceptor molecules as r^{-6}. This is a short-range process taking place on a distance range from subnanometers to several nanometers. Therefore, the annihilation rate coefficient is determined by the microscopic material properties. In case of conjugated polymers, such properties are intersegment distances and their orientation, the ground state and excited state absorption, stimulated emission cross sections, and their spectra. On the contrary, ASE is a long-range process determined by the radiative energy transfer. The rate of this process depends on the distance as r^{-2}. Due to the long-range transfer character, the ASE properties depend on the macroscopic parameters of samples like the film thickness and shape [3,4].

In this work, we study the exciton-exciton annihilation and ASE properties in a poly(para-phenylene)-type ladder polymer (m-LPPP). This polymer is an effective emitter in the blue spectral region. It shows more that 85% fluorescence quantum yield in solutions and up to 25% in solid films. It is one of the best blue emitting materials for polymeric light emitting diodes and also has high potential for the application as a polymeric laser material. The nonlinear relaxation processes become particular important in case of the laser application.

EXPERIMENTAL

m-LPPP was synthesized as described in Ref. [7], and the polymer films were deposited on glass or indium-tin oxide (ITO) covered glass by spin coating from a toluene solution (1% by weight). The polymer film thickness was about 100 nm, and the films had the optical density at the maximum of the visible absorption band of about 0.8.

Investigations were performed by the absorption pump-probe technique with femtosecond time resolution. The samples were excited by about 50-fs pulses of a non-collinear parametric generator pumped by frequency-doubled pulses generated by a Ti:sapphire laser. Variable wavelength pulses generated by another non-collinear parametric generator probed the differential absorption. The spectrometer enabled a very high measurement accuracy with a standard deviation of less than 10^{-4} in the differential absorption signal per pair of probe pulses with and without excitation.

RESULTS AND DISCUSSION

The transient absorption kinetics in m-LPPP films at high excitation intensities is very sensitive to the presence of additional layers like ITO or metal. Figure 1 shows the transient absorption relaxation at different wavelengths in the presence and absence of an ITO layer. In the presence of the ITO layer (Fig. 1a), the transient absorption relaxes gradually at all probe wavelengths. However, the relaxation kinetics at different wavelengths is different. The slow relaxation component is evident at all probe wavelengths, except for a probe at 496 nm. This slow component should be related to the generation of charge pairs which have much longer lifetime than excitons [8]. Excitons and polymer segments in the ground state have equal absorption cross-sections at 496 nm. Therefore, the probe at this wavelength adequately reflects the exciton relaxation kinetics. Thus, we used this probe wavelength to monitor the exciton kinetics.

As will be discussed later, ITO and metal layers prevent the development of ASE [6]. Therefore, we will discuss, at first, the relaxation kinetics determined in the presence of an ITO layer, when ASE makes no influence.

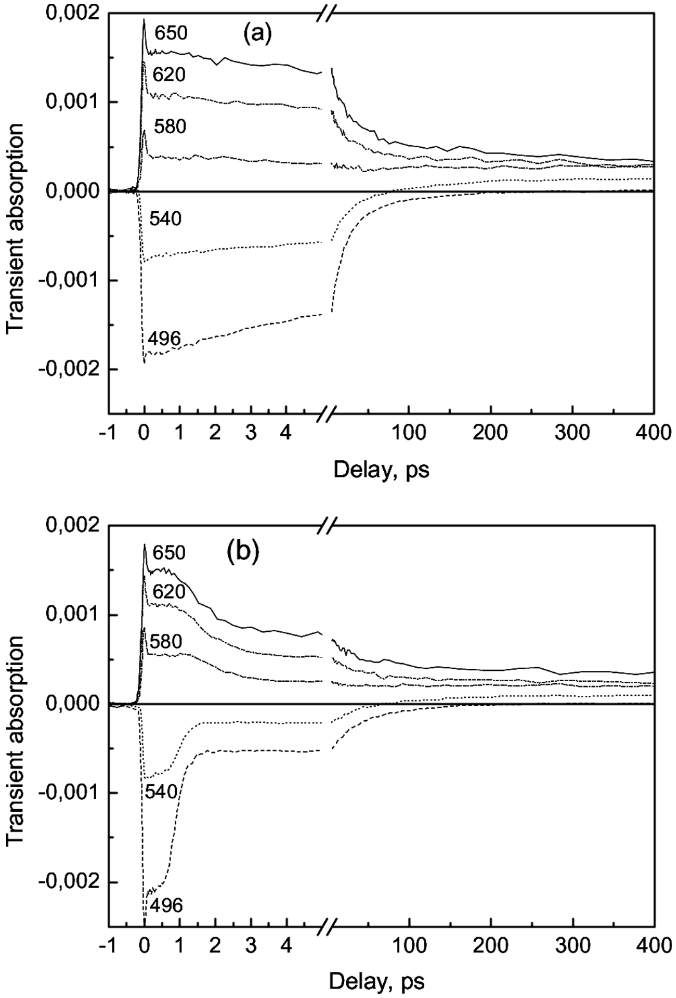

FIGURE 1 Transient absorption relaxation of an m-LPPP film measured at different probe wavelengths.

Figure 2 shows the transient absorption kinetics measured at 496 nm under varied excitation intensities. The right axes of the graph shows the relative exciton density, i.e., the ratio of the exciton density to the total conjugated segment density. This value is related to the transient absorption intensity by the following relation

$$\frac{n^*}{N} = \frac{\Delta A}{A}\frac{\sigma_{ab}}{\sigma^* - \sigma_{ab} - \sigma_{em}}, \tag{1}$$

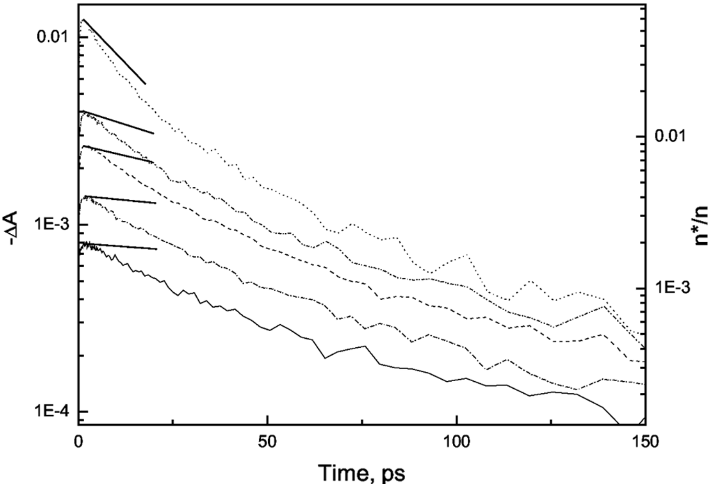

FIGURE 2 Absorption bleaching kinetics of an m-LPPP film measured at 496 nm under excitation at 447 nm by 0.8, 0.5, 0.2, 0.1, and 0.03 mJ/cm^2 intensity pulses. Straight lines indicate the initial exciton-exciton annihilation rates.

where σ_{ab}, σ_{em}, and σ^* are the absorption, stimulated emission, and excited state (exciton) absorption cross sections, respectively. σ_{em} may be calculated from the fluorescence spectrum, and σ^* was estimated from the transient absorption spectra (not shown). The exciton density decay in films is nonexponential (nonlinear on the ln scale) even at the lowest excitation intensities. Additionally, the fast relaxation component, which should be attributed to the exciton-exciton annihilation, appears with increasing the excitation intensity.

The exciton decay in the presence of annihilation can be expressed as

$$\frac{dn^*}{dt} = -k(t)n^* - \gamma(t)n^{*2}, \tag{2}$$

where *k(t)* is the linear relaxation rate (reciprocal exciton lifetime) and $\gamma(t)$ is the annihilation rate. Since the two lowest excitation intensities curves are almost identical, we can assume that the lowest intensity curve is almost unaffected by the annihilation. Subtracting it from the highest intensity curve, we obtain the initial annihilation rate at the highest excitation intensity. According to relation (2), the annihilation rate is proportional to $\gamma_{t=0}n$. Thus, we can estimate it for the relaxation kinetics obtained at lower intensities. The estimation values are shown in Figure 2 by straight lines. The initial annihilation rate corresponds to the slope of the lines. In agreement with our previous assumption, the annihilation rate for the lowest intensity curve is much lower than the intrinsic relaxation rate, while the annihilation dominates at the highest intensity. This indicates that the sizeable influence of the exciton-exciton annihilation on the relaxation kinetics starts at a relative exciton density of about 10^{-3}.

We can also determine the time dependence of the annihilation rate. By dividing both sides of Eq. (2) by n^* and signing $K = (1/n^*)(dn^*/dt)$, which is the exciton relaxation rate, we can express the annihilation rate as

$$\gamma(t) = -(K - k(t))/n^*. \tag{3}$$

Since the intrinsic linear relaxation rate is also unknown, we can find both these parameters from the relaxation kinetics at two different excitation intensities:

$$\begin{aligned} \gamma(t) &= -\frac{K_1 - K_2}{n_1^* - n_2^*} \\ k(t) &= -\frac{K_1 n_2^* - K_2 n_1^*}{n_1^* - n_2^*}, \end{aligned} \tag{4}$$

where subscripts 1 and 2 correspond to the respective values at different intensities.

Figure 3 shows the obtained annihilation rates in an m-LPPP film obtained for three curve pairs of different intensities. Despite the relatively large errors caused by differentiation of the experimental decay curves, two important features can be observed. First, the time dependences of these values obtained from the different kinetic pairs are identical within experimental errors. This supports the validity of the applied approach. Second, the annihilation rate is time independent within the experimental accuracy, at least on the time scale of tens of ps, and equals to about $1.3^* 10^{-8}\,\mathrm{s}^{-1}\,\mathrm{cm}^3$. The time independent exciton annihilation rate is not what was expected. There are the processes such as static annihilation, low-dimensional exciton diffusion, exciton trapping, etc. that lead to a decrease annihilation rate in time. The annihilation with time-dependent rate was observed in different molecular materials, such as phthalocyanines [9] or columnar phases of liquid crystals [10]. The time-independent annihilation rate indicates that none of the above-listed factors makes a strong influence on the exciton annihilation rate.

Now let us discuss the properties of ASE. The transient absorption kinetics in samples without ITO has very different shapes (see Fig. 1b). During the first initial picosecond, the relaxation kinetics in the samples with and without ITO are almost identical. However, later on, a very fast partial decay takes place in the sample without ITO,

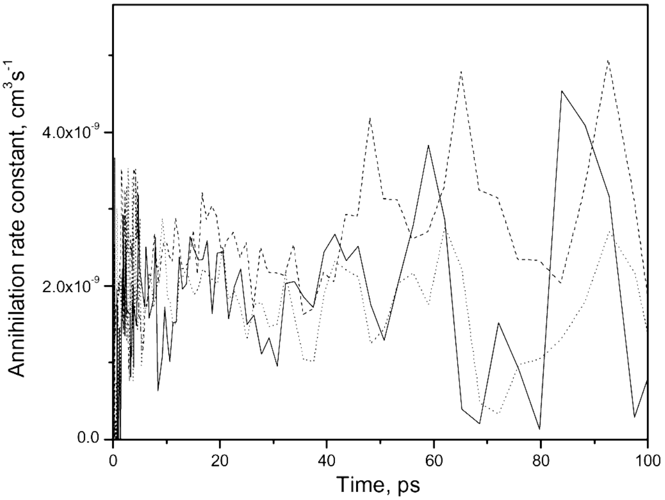

FIGURE 3 Time dependence of the exciton-exciton annihilation rate coefficient in an m-LPPP film obtained from three different pairs of transient absorption kinetics measurements at 496 nm under different excitation intensities at 447 nm.

while the subsequent subnanosecond decay is almost identical again. The rapid decay is observed at all probe wavelengths. Such behaviour shows that the ASE taking place in sample without ITO layer is responsible for the observed differences. Thus, ASE evidently rapidly reduces the exciton concentration and, however, does not influence the charge pair generation and relaxation.

Figure 4 compares the transient absorption relaxation kinetics measured under different intensity excitations in m-LPPP films with ITO (*a*) and without it (*b*). The kinetics was measured at 496 nm, where only excitons are responsible for the transient absorption signal. The slow component is dominant in samples with ITO independently of the excitation intensity. The kinetics measured at the lowest excitation intensity is almost identical in samples with and without ITO. However, a clear rapid relaxation component appears in the sample without ITO by increasing the excitation intensity just by 1.5 times. The further increase in the excitation intensity leads to the even more pronounced rapid relaxation. Moreover, the delay time of the observed abrupt signal drop decreases with increasing the excitation intensity, and it leads even to the signal decrease at the delay time of about 2 ps. At longer delay times, the relaxation kinetics and the transient absorption intensity are perfectly independent of the

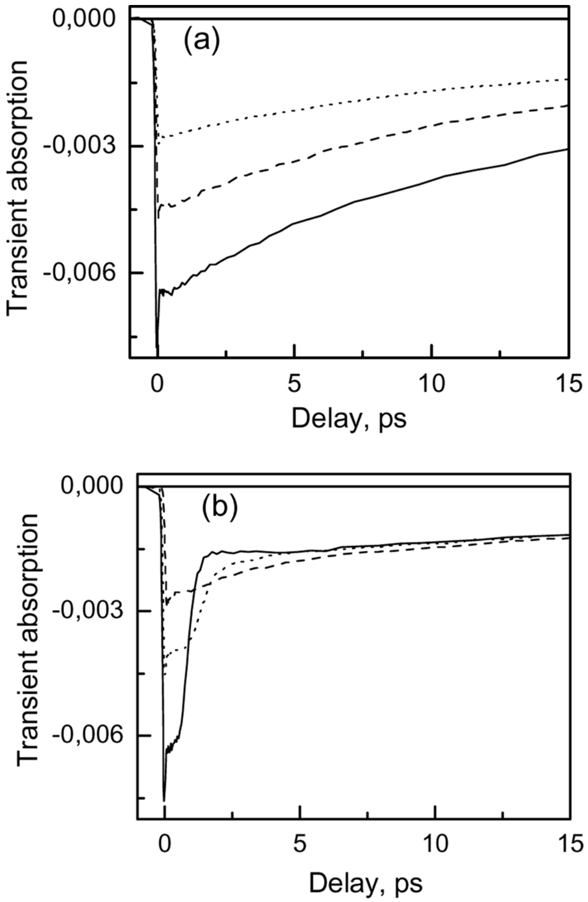

FIGURE 4 Transient absorption relaxation kinetics in m-LPPP films with ITO layer (a) and without ITO (b) measured at 496 nm under excitation by 0.2, 0.3, and 0.6 mJ/cm^2 intensity pulses.

excitation intensity. Thus, ASE results in a very unusual relaxation kinetics. The appearance of ASE is evident by visual observation, too. Figure 5 shows the spatial distribution of the film luminescence under identical excitation conditions in the areas of samples covered- and uncovered- by ITO. The fluorescence spot in the ITO-covered area is sharp with clear boundaries. The fluorescence spot from the uncovered area is wider and has no clear boundaries. The difference in the fluorescence appearances is related to the stimulated emission light propagation in the waveguide formed by a polymer film. The

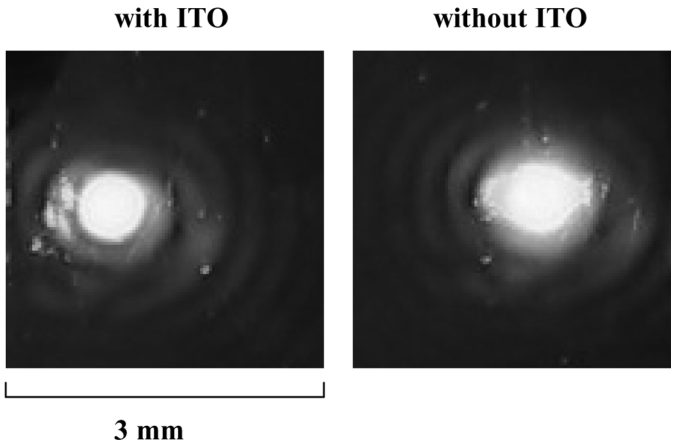

FIGURE 5 Spatial distribution of the film luminescence intensity obtained under identical excitation conditions in the sample areas covered and noncovered by ITO.

fluorescence spot widening gives us an estimate of the light propagation distance which is of the order of hundred micrometers.

Figure 6 explains the ASE mechanism. A photon generated by the spontaneous emission propagates along the sample. Photons propagating at large angles relative to the film surface leave the sample, while those propagating at low angles enter the plane waveguide mode formed by the polymer film surfaces. Light propagating in the waveguide mode is amplified due to the stimulated emission by other excitons in the film. Since the film thickness is much smaller than the light wavelength, the waveguide mode is not confined inside the polymer film. It enters ITO or metal layers if they are formed next to the film. Because of the strong light absorption inside the ITO or metal layers, the waveguide mode is dumped and ASE cannot develop or its development threshold significantly increases [6].

In contrary to the exciton annihilation which depends only on the exciton density, the ASE dynamics depends on two parameters, the exciton and photon densities. They may be described by the rate equations

$$\frac{dn^*}{dt} = -[k_{rad}(t) + k_{non}(t)]n^* - \gamma(t)n^{*2} - \chi n^* f, \tag{5}$$

$$\frac{df}{dt} = k_{rad}(t)n^* + \chi n^* f - \frac{1}{\tau} f \tag{6}$$

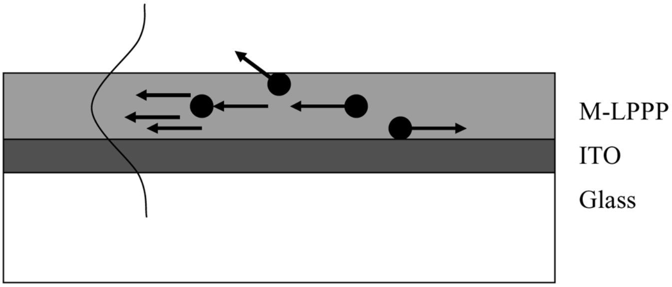

FIGURE 6 ASE formation mechanism.

Here, f is the photon density, τ is the average photon residence within polymer film time, and χ expresses the stimulated emission event probability. Let us shortly analyze the rate equations. The first two terms in Eq. (5) express the intrinsic exciton relaxation and their annihilation, while the third term expresses the exciton decay due to the stimulated emission. The photon generation is determined by the first term of Eq. (6) which expresses the radiative exciton decay and by the second term due to the stimulated emission. The photon onset and, consequently, the fast exciton decay start when the second term exceeds the first one: $\chi n^* f > k_{rad}(t)n^*$. At this time moment, the avalanche photon generation starts. When the exciton and, consequently, photon densities drop down, so that $\chi n^* f < k_{rad}(t)n^*$, the avalanche photon generation stops and ASE does not influence the exciton relaxation kinetics any more. Thus, ASE finally stabilizes the exciton density to the value determined by the ASE threshold and independent of the excitation intensity. The ASE process has a threshold-like excitation intensity dependence. If the excitation intensity is not sufficient to reach the necessary photon density, the ASE does not develop.

Our experimental data show that both the nonlinear processes of exciton-exciton annihilation and ASE start at similar excitation intensities. However, this is the accidental coincidence, since ASE threshold depends, as was mentioned, on the geometric parameters of a sample, as well as on such factors as the film surface flatness, the presence of light absorbing and scattering centers in the polymer, etc.

CONCLUSIONS

Our experiments show that two nonlinear exciton relaxation processes, the exciton-exciton annihilation and amplified spontaneous emission, can influence the exciton relaxation kinetics at high excitation intensities. Although both processes under certain experimental conditions can become apparent at similar excitation intensities, their properties and consequences are very different.

REFERENCES

[1] Sundstrom, V., Gilbro, T., Gadonas, R., Piskarskas, A. (1988). *J. Chem. Phys.*, *89*, 2754.

[2] Markovitsi, D., Lecuyer, I. (1991). *J. Chem. Phys.*, *95*, 3620.

[3] Cerullo, G., Stagira, S., Nisoli, M., De Silvestri, S., Lanzani, G., Kranzelbinder, G., Graupner, W., Leising, G. (1998). *Phys. Rev.*, *57*, 12806.

[4] Nisoli, M., Stagira, S., Zavelani-Rossi, M., De Silvestri, S., Mataloni, P., Zenz, P. (1999). *Phys. Rev.*, *59*, 11328.

[5] Haugeneder, A., Neges, M., Kallinger, C., Spirkl, W., Lemmer, U., Feldmann, J., Amann, M. C., Scherf, U. (1999). *J. Appl. Phys.*, *85*, 1124.

[6] Reufer, M., Feldmann, J., Rudati, P., Ruhl, A., Müller, D., Meerholz, K., Karnutsch, C., Gerken, M., Lemmer, U. (2005). *J. Appl. Phys.*, *86*, 221102.

[7] Sherf, U., Bohnen, A., Müllen, K. (1992). *Macromol. Chem. Phys.*, *193*, 1127.

[8] Müller, J. G., Lemmer, U., Feldmann, J., Scherf, U. (2002). *Phys. Rev.*, *88*, 147401.

[9] Gulbinas, V., Chachisvilis, M., Valkunas, L., Sundström, V. (1996). *J. Phys. Rev.*, *100*, 2213.

[10] Markovitsi, D., Lecuyer, I. (1991). *J. Chem. Phys.*, *95*, 3620.